Fast screening of Depolymerized Lignin Samples Through 2D-Liquid Chromatography Mapping

Tibo De Saegher,[a] Jeroen Lauwaert,*[a] Joeri Vercammen,[a, b] Kevin M. Van Geem,[c] Jeriffa De Clercq,[a] and An Verberckmoes[a]

Lignin valorization and particularly its depolymerization into bio-aromatics, has emerged as an important research topic within green chemistry. However, screening of catalysts and reaction conditions within this field is strongly constrained by the lack of analytical techniques that allow for fast and detailed mapping of the product pools. This analytical gap results from the inherent product pool complexity and the focus of the state-of-the-art on monomers and dimers, overlooking the larger oligomers. In this work, this gap is bridged through the development of a quasi-orthogonal GPC-HPLC-UV/VIS method that is able to separate the bio-aromatics according to molecular weight (hydrodynamic volume) and polarity. The method is evaluated using model compounds and real lignin depolymerization samples. The resulting color plots provide a powerful graphical tool to rapidly assess differences in reaction selectivity towards monomers and dimers as well as to identify differences in the oligomers.

1. Introduction

In recent years, chemistry and chemical engineering research has been strongly focusing on replacing fossil resources by sustainable alternatives.[1–3] As it is the cheapest and most abundantly available inedible biomass, lignocellulosic biomass is commonly recognized as the most scalable and economically viable bio-source to produce both bio-fuels and high value chemicals.[3–9] Lignocellulose consists of three highly functional biopolymers, namely cellulose, hemicellulose and lignin. The latter consists of functionalized aromatic building blocks, which are linked through mostly ether (C–O) and, to a lesser extent, carbon-carbon (C–C) bonds, making it the largest renewable source of aromatics.[7,10,11] As a result, lignin depolymerization into functionalized bio-aromatics, i.e., monomers, dimers and oligomers, will become the main bio-based route towards sustainable aromatic chemicals and building blocks for polymer synthesis or other high value applications.[5,11–18] Unfortunately, most polysaccharide focused industries discard lignin as a waste product. As a result, an estimated 100 million tonnes of lignin (technical lignins), mainly coming from the paper and pulping industry, is annually burned as low value fuel.[5] Hence, further improvements in the field of lignin depolymerization are crucial to unlock the full potential of lignin at the industrial scale.

Various depolymerization strategies, of varying nature, i.e., biochemical or chemical, have been investigated. Among the biochemical routes, enzymes such as laccase have been used to selectively cleave lignin C–O linkages to produce functionalized bio-aromatics.[19–21] Chemical strategies such as solvolysis, mild reductive depolymerization and mild oxidative depolymerization also target selective cleavage of C–O linkages within lignin through different reaction mechanisms, which leads to differences in the resulting product pools. For example, mild oxidative depolymerization pathways mainly pass through ketonic intermediates and result in the oxidation of functional groups, yielding high amounts of aldehydes ((C=O)H), ketones ((C=O)C) and carboxylic acids ((C=O)OH).[15,22–28] More specifically, vanillin (**V**) is one of the most interesting and relevant aldehydes derived from lignin for the polymer industry.[29] In contrast, products obtained after mild reductive depolymerization under hydrogen atmosphere contain a higher number of hydroxyl functional groups (OH) and, comparatively, display the highest selectivity towards functionalized aromatics.[15,30–32] Moreover, if a protic solvent, e.g., alcohols, is used as the only hydrogen source, i.e., solvolysis or catalytic liquid phase reforming under inert atmosphere, a relatively lower product selectivity is reached due to the increased complexity of the reaction pathways and incorporation of the solvent into the final products.[33–37]

Despite of these crucial observations, lignin depolymerization research is hindered by the lack of appropriate analysis techniques that allow fast and detailed assessment of the chemically diverse product pools to assist catalyst development and reaction conditions optimization. The absence of such techniques is mainly caused by the immense variability in

[a] T. De Saegher, Dr. J. Lauwaert, Prof. J. Vercammen, Prof. J. De Clercq, Prof. A. Verberckmoes
Department of Materials Textiles and Chemical Engineering (MaTCh)
Ghent University
Valentin Vaerwyckweg 1, 9000 Ghent (Belgium)
E-mail: Jeroen.Lauwaert@UGent.be
[b] Prof. J. Vercammen
Interscience Expert Center (IS-X)
Avenue J.E. Lenoir 2, 1384 Louvain-la-Neuve (Belgium)
[c] Prof. K. M. Van Geem
Department of Materials Textiles and Chemical Engineering (MaTCh)
Ghent University
Technologiepark 125, 9052 Ghent (Belgium)

ChemistryOpen

Full Papers
doi.org/10.1002/open.202100088

**Chemistry
Europe**
European Chemical
Societies Publishing

linkage types and functional groups within lignin, giving rise to a proportional chemical complexity in the product pool, even when selective depolymerization strategies are applied. Although very powerful gas chromatography (GC) techniques exist, particularly when applied in a multidimensional set-up, they require drastic procedures, such as chemical derivatization or analytical pyrolysis to cope with the low volatility of the components in the product pools (most dimers, trimers and oligomers).[8,30,38–41] Moreover, both procedures complicate identification and require complex data analysis protocols. As a consequence, the resulting techniques lack the speed, conciseness and cost effectiveness required for rapid catalyst development and optimization of reaction conditions.[42] In that respect, high performance liquid chromatography (HPLC) is much more suitable, but comprehensive characterization of the entire product pool is not possible in a single run without complex detection techniques, such as tandem mass spectrometry (MS) to elucidate co-eluting components, again reducing the speed and conciseness of the analysis technique.[43,44] Therefore, although powerful, these techniques are highly time-intensive and convoluted for the initial stages of catalyst screening and optimization of reaction conditions, i.e., where a large number of variations have to be rapidly analyzed and compared. Gel permeation- or size exclusion chromatography (GPC or SEC) is often used to quickly examine the molecular weight distribution within the complete product pool.[30,40] However, translating hydrodynamic volume to molecular weight, especially for lower molecular weight fractions, is prone to errors due to solvent effects, non-steric interactions and the lack of representative standards.[30,45,46] Therefore, although GPC or SEC is able to deliver concise data in a reasonable timeframe, it is not detailed enough for practical catalyst screening or reaction conditions optimization. In conclusion, the development of an analysis technique, capable of quickly providing detailed information regarding the nature of both lower and higher molecular weight compounds in a concise, preferably graphical manner, is crucial for the optimization of lignin depolymerization and, hence, lignin valorization.

In this work, an analytical method, capable of quickly providing sufficiently detailed information regarding the relative composition and nature of both lower and higher molecular weight compounds in a concise and graphical manner is presented. Due to the inherent complexity of lignin depolymerization products, generated by both the number of compounds and their structural similarities, a two-dimensional separation approach is mandatory.[47] Moreover, this complexity requires high peak capacity in the second dimension (^{2}D). Therefore, a multiple heart cutting (mLCxLC) setup, i.e., ^{2}D analysis of a well-selected series of successive fractions from the first dimension (^{1}D), is preferred over a full comprehensive (LCxLC) method to maximize ^{2}D resolution while limiting the overall analysis time.[47] More specifically, in this work, a mLCxLC GPC-HPLC-UV/VIS technique has been developed. Both ^{1}D and ^{2}D target crucial characteristics of the reaction products for reaction conditions optimization, catalyst development as well as the valorization of the products within the polymer industry, namely molecular weight and functionality, respectively. A

similar offline GPCxHPLC setup has been utilized before to analyze samples of a thermochemical and biochemical conversion of lignocellulosic biomass, i.e., containing both polysaccharides and lignin.[46] However, in the work presented here, a column modified with polar cyano (CN) groups is evaluated for the ^{2}D, as, in contrast to the commonly used C18 columns,[46] such a column is able to induce selective interactions towards OH-groups, the most important functionality for valorization in the polymer industry, on ^{2}D retention time (^2t_R). Moreover, only samples containing low molecular weight lignin monomers and a limited number of dimers have been considered up till now.[46] Hence, in this work, this type of technique is, for the first time, implemented for the dedicated analysis of entire lignin depolymerization product pools.

2. Results and Discussion

2.1. Model Compound Analysis

Identification of the model compounds (MC), of which the structures and respective abbreviations are presented in Figure 1, in the 2D color plot of the GPC-HPLC-UV/VIS analysis of the standard mixture, is executed through their respective ^{2}D-retention time, which was determined a priori by injection of one or two MCs onto HPLC (i.e., ^{2}D of the GPC-HPLC-UV/VIS technique) directly. Therefore, several HPLC analyses of samples containing 100 mg/L of either 1 or 2 MCs in dimethylsulfoxide (DMSO), were performed. A superposition of the resulting ^{2}D chromatograms and accompanying identification of the model compounds is shown in Figure 2.

Firstly, Figure 2 clearly illustrates that several MCs would co-elute if injected onto ^{2}D as a mixture, namely, **EV** and **SA**, **TFA** and **GG** and **4PP** and **PPE**, necessitating an additional dimension for separation. As most co-eluting MCs, except **4PP**
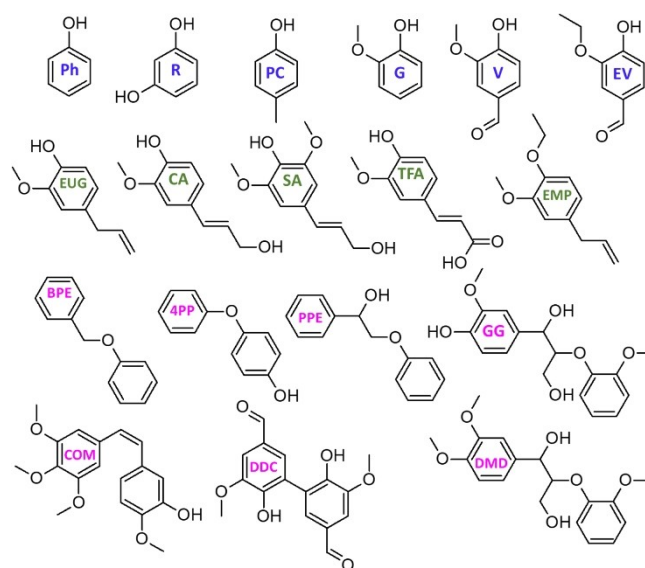
Figure 1. Molecular structure and corresponding abbreviations of the phenolic (blue), eugenolic (green) and dimeric (violet) model compounds
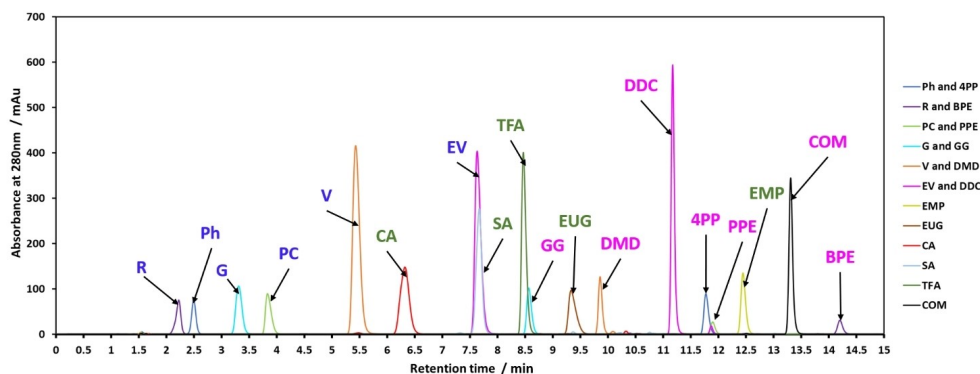
ChemistryOpen

Full Papers
doi.org/10.1002/open.202100088

Chemistry Europe
European Chemical
Societies Publishing

Figure 2. Superposition of the HPLC-UV/VIS (^{2}D) chromatograms of all model compound mixtures with accompanying identification of the model compounds

and **PPE**, differ significantly in molecular weight and functional groups, GPC is a good candidate for a secondary dimension as its separation is based on hydrodynamic volume and, hence, closely related to differences in molecular weight and functional groups.[30,45,46] Additionally, the effect of functional groups in ^{2}D can be summarized accordingly: while methoxy (**Ph** to **G** and **CA** to **SA**), ethoxy (**V** to **EV** and **EUG** to **EMP**), alkyl/alkenyl (**Ph** to **PC** and **G** to **EUG**) and aldehyde groups (**G** to **V**) increase ^2t_R, OH-groups (**Ph** to **R**, **BPE** to **4PP/PPE** and **DMD** to **GG**) and, to a lesser extent, COOH-groups (**EUG** to **TFA**) decrease ^2t_R. A listing of these effects can also be found in Table 1. Notably, this trend indicates that the effect of OH-groups, one of the primary characteristics for valorization in the polymer industry, on ^2t_R is

distinctly opposite to most other functional groups, with COOH being the only exception.

With the ^2t_R of all MCs elucidated, serving as a major identification parameter, a mixture containing 2000 mg/L of all 18 MCs, diluted in DMSO, was analyzed with the GPC-HPLC-UV/VIS method. The GPC-UV/VIS (^{1}D) chromatogram of the MC mixture, with indication of the 11 fractions subsequently analyzed with HPLC-UV/VIS (^{2}D), is presented in Figure 3. Set chromatogram indicates that the MCs are separated to a limited extent in the first dimension of the 2D technique with most peaks eluting between a ^1t_R of 20.5 min and 23.5 min. However, a notable exception is the peak between a ^1t_R of 18.5 min and 19 min. This discrepancy is likely caused by a rigid structure and/or the aforementioned solvent effects and non-steric interactions during GPC analysis, which have been noted in literature.[30,45,46] Analysis of the ^{1}D-fractions in Figure 3 by means of HPLC-UV/VIS in the second dimension allows for identification of the MC(s) responsible for this extraordinary peak as well as the other ones.

The 2D color plot for the MC mixture, with identification of the model compounds, is presented in Figure 4. The identification is based on their respective ^2t_R elucidated in Figure 2. The
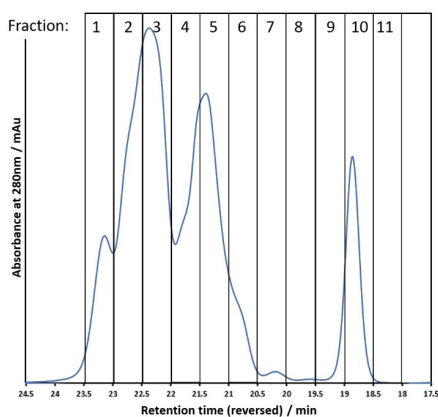
Table 1. Different functionalities and their respective effect on ^{2}D retention time.

Functionality	Effect on ^{2}D retention time
—OH	↓↓
—OCH$_3$, —OCH$_2$CH$_3$	↑
—R/—RCH=CH—R'	↑↑
—(C=O)H	↑
—(C=O)OH	↓

Figure 3. GPC-UV/VIS-chromatogram of the model compound (MC) mixture, containing the 18 compounds with a concentration of 2000 mg/L, with indication of the 11 fractions analyzed in ^{2}D.
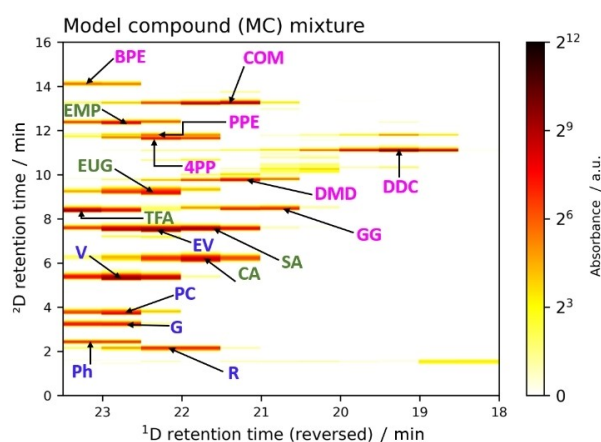

Figure 4. 2D color plot for the GPC-HPLC-UV/VIS analysis of the MC mixture with accompanying identification of the model compounds.

ChemistryOpen

Full Papers
doi.org/10.1002/open.202100088

Chemistry Europe
European Chemical
Societies Publishing

^{2}D chromatograms of all ^{1}D-fractions are represented in Figure S1 in the Supporting Information. Regarding ^{1}D, less functionalized dimers such as **BPE**, **4PP** and **PPE** elute at similar ^{1}D retention times (^1t_R) to most monomers (such as **R**, **Ph**, **G**, **PC**, etc.). However, highly functionalized, lignin-like dimers (**GG**, **DMD**, **COM** and **DDC**) exhibit a much lower ^1t_R, indicating that the ^{1}D separation is not strictly SEC-based for lignin derived compounds, which is in line with literature.[30,46] As a guideline, the color plot for the MC mixture indicates that ^1t_R reduces with increasing hydrodynamic volume and/or reduction of the C/O-ratio. The former causes **DDC**, a dimeric compound with the rigid 5–5 biphenyl linkage, to elute at a far lower ^1t_R, compared to other dimeric MCs, hence, being responsible for the aforementioned, unique peak in the GPC-UV/VIS chromatogram in Figure 3 (18.5 min–19 min) while, based on the latter, coelution of substrates with vastly different hydrodynamic volume can be expected. Moreover, an increase in the number of OH-groups seems to result in the largest reduction of ^1t_R as evident in both monomeric (**Ph** to **R** and **EUG** to **CA**) and dimeric (**BPE** to **PPE**/**4PP** to **DMD** to **GG**) regions. This trend corresponds to a separation based on hydrophobicity superimposed on top of the size exclusion mechanism, which is confirmed by increased ^1t_R of the less functionalized dimers (**BPE**, **4PP** and **PPE**) as mentioned above. While the aromatic rings in lignin are sufficiently functionalized to negate this, side reactions during mild depolymerization such as hydrodeoxygenations or ester- and etherifications could remove functionalities, thus, leading to, at first sight unexpectedly, high ^{1}D retention times.[15,30,33] The application of ^{2}D compensates for this effect as ^2t_R is significantly increased through the addition of alkyl/alkenyl groups (**Ph** and variants to **EUG** and variants) and/or aromatic systems (**GG**, **DMD**, **DDC**, **COM**, **4PP**, **PPE**, **BPE**), creating specific zones in ^{2}D. Still, differences in functional groups can cause these zones to overlap and, hence, lead to coelution in ^{2}D, which, in turn, necessitates the first dimension. In general, the combination of ^{1}D and ^{2}D results in adequate separation of all model compounds.

All MCs that would coelute if directly injected onto ^{2}D, indicated in Figure 2, are now separated in the 2D-plot through the addition of ^{1}D, the only exceptions being **PPE** and **4PP**, both eluting in fraction 3. However, if observed closely (also see Figure S1 in the Supporting Information), the two peaks corresponding to these MCs can still be distinguished in ^{2}D, despite being near structural isomers with the same number of aromatic moieties and one common functional group, demonstrating the high resolving power of the 2D method. Furthermore, the fact that **4PP** and **PPE** lack additional functional groups results in a unique ^{1}D and ^{2}D retention compared to lignin-like products such as **COM**, **DMC**, **DDC** and **GG**. The elution of peaks in this area, i.e., ^{1}D fractions 1–4 and ^{2}D retention time of >11 min, is a useful indicator for unwanted side reactions that remove OH-groups. Moreover, the GPC-HPLC-UV/VIS method is very sensitive towards the number of OH-groups in both dimensions, i.e. an increase in the average number of OH-groups will cause a shift of the product pool to lower ^1t_R and ^2t_R.
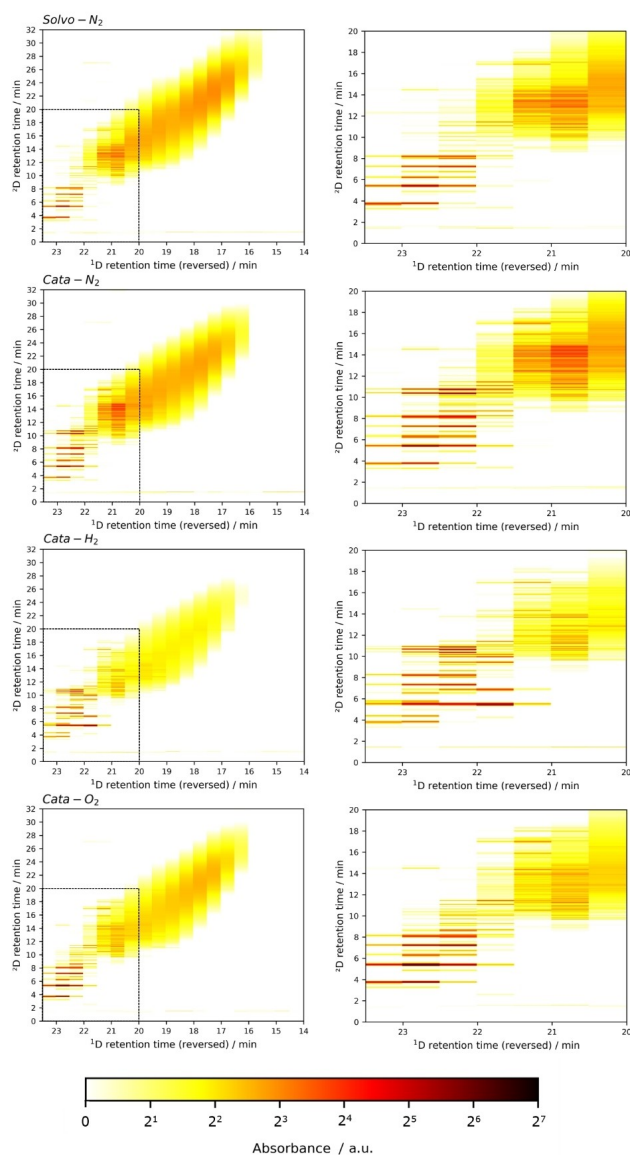
2.2. Depolymerization Effluent Analysis

The GPC-UV/VIS (^{1}D) chromatograms of all depolymerization effluents are presented in Figure 5 and already reveal differences in depolymerization degree and product selectivity. Cata-H$_2$ displays a slightly lower absorbance at 280 nm throughout the entire ^{1}D chromatogram. However, the hydrogenation of aliphatic and aromatic C=C bonds under mild reductive conditions has been observed and could explain this difference in overall intensity.[15,48,49] Secondly, while all samples display distinct peaks between 20 min–21 min and 21.5 min–23 min, the peak shape and relative intensities differ amongst the samples. Moreover, only Cata-H$_2$ is characterized by an additional peak around 21.5 min, indicating a unique product selectivity within the product pool. Additionally, while no distinct peaks can be distinguished at ^1t_R lower than 19.5 min, differences in the GPC-UV/VIS chromatograms between the depolymerization effluents can still be noted, i.e., shape and height. In conclusion, GPC-UV/VIS analysis of the depolymerization product pools enables identification of compositional differences but a second dimension is needed to assess the nature of these differences. Therefore, the complete GPC-UV/VIS (^{1}D) effluents of all samples were collected in 19 fractions of 0.5 min (0.4 ml) between a ^1t_R of 14 min and 23.5 min and analyzed with HPLC-UV/VIS (^{2}D). The ^{1}D-fractions are labelled 1 through 19 in reverse order, starting with the 23–23.5 min fraction as indicated in Figure 5.

The 2D color plots for the entire effluent of Solvo-N$_2$, Cata-N$_2$, Cata-H$_2$ and Cata-O$_2$ are presented in Figure 6 with accompanying subplots, focusing on the bottom left quadrant
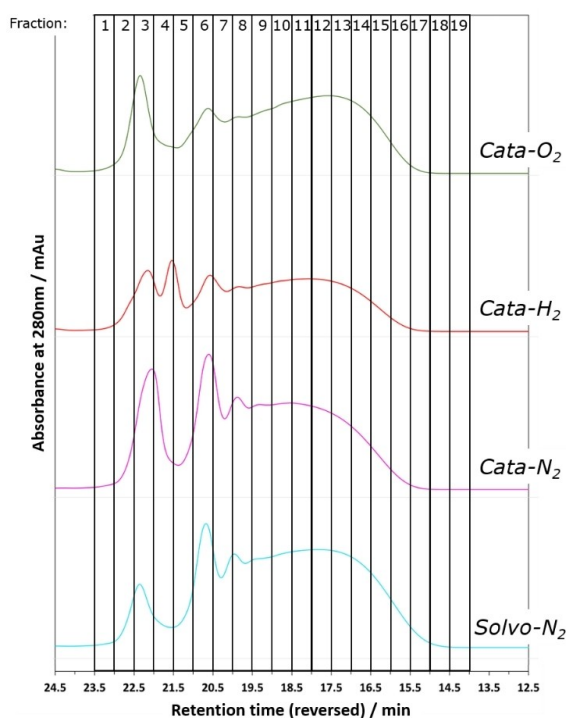
Figure 5. GPC-UV/VIS-chromatograms of Solvo-N$_2$, Cata-N$_2$, Cata-H$_2$ and Cata-O$_2$ with indication of the 19 fractions analyzed in ^{2}D.

ChemistryOpen

Full Papers
doi.org/10.1002/open.202100088

**Chemistry
Europe**
European Chemical
Societies Publishing

Figure 6. GPC-HPLC-UV/VIS color plots of the entire effluent (left) for the Solvo-N_2 (row 1), Cata-N_2 (row 2), Cata-H_2 (row 3) and Cata-O_2 (row 4) samples with accompanying subplots (right), focusing on the bottom left quadrant of the complete plots.

of the complete plots. The individual ^{2}D-chromatograms of all fractions can be found in Figures S2 and S3 in the Supporting Information. The GPC-HPLC-UV/VIS color plots, depicted in Figure 6, clearly illustrate the efficacy of the technique for fast, detailed and graphical compositional screening of lignin depolymerization samples. The separation space is adequately utilized, considering the reasonable orthogonality of GPC and RP-HPLC, both inherent to the separation modes and a consequence of the aforementioned effect of hydrophobicity on ^{1}t$_R$.[50] Moreover, the increase in ^{2}t$_R$ with decreasing ^{1}t$_R$, creating the diagonal nature of the product distribution throughout the color plot, is in accordance with the results of

MC as it demonstrated that the addition of aromatic moieties significantly increases ^{2}t$_R$.

Additionally, the number of peaks increases and, hence, the resolution decreases at lower ^{1}D retention times. This is expected as the number of potentially different components increases exponentially with increasing aromatic chain length. As a consequence, regions of high peak density are observed in all samples at low ^{1}t$_R$. However, important differences between the samples remain notable in these regions, indicating that the application of the proposed GPC-HPLC-UV/VIS method is not limited to monomers and dimers and, thus, significantly advances beyond the state-of-the-art.[46] For example, Solvo-N_2 and, especially, Cata-N_2 are characterized by relatively intense peaks within ^{1}D-fraction 6 (20.5 min–21 min), see the subplots within Figure 6, which are absent in the other samples. More-over, these types of differences cannot be elucidated from the GPC-UV/VIS chromatograms in Figure 5 and therefore, demon-strate the efficacy of the two-dimensional approach. Addition-ally, the Cata-H_2 product pool exhibits a region of high peak density which is smaller and located at lower ^{1}t$_R$ and ^{2}t$_R$ compared to the other product pools, more clearly visualized in Figure S3 in the Supporting Information. The former indicates a narrower distribution of functionalities, while, based on the results for MC, the latter implies a higher concentration of OH-groups in the product pool which is, as aforementioned, expected for product pools obtained via reductive depolymerization.[15,30–32] Moreover, the relative sizes and loca-tions of the regions with high peak density also demonstrate that the Cata-H_2 shows the highest degree of depolymerization.

The unique composition of the Cata-H_2 sample continues within the region of low peak density, depicted within the subplots in Figure 6. Firstly, the transition from low to high peak density, more clearly illustrated in the subplots in Figure 6, is the most discrete within the Cata-H_2 sample, displaying a drastic shift in ^{2}t$_R$ from ^{1}D-fractions 4 to 5, i.e., ≤ 12 min to ≥ 10 min, respectively. In all other samples, this transition is more subtle, showing numerous minor peaks with a ^{2}t$_R > 12$ min in ^{1}D-fractions 4 and 3. Denoting peaks within the depolymeriza-tion effluents which correspond to model compounds (based upon the agreement of both ^{1}t$_R$ and ^{2}t$_R$), as demonstrated in Figure S5 in the Supporting Information, strongly indicates that the peaks with a ^{2}t$_R > 12$ min in ^{1}D-fractions 4 and 3 can be attributed to less functionalized dimeric species, formed through unwanted side reactions, hence, further confirming the high selectivity of the Cata-H_2 sample. Moreover, Solvo-N_2 and Cata-N_2 exhibit peaks at the ^{1}t$_R$ and ^{2}t$_R$ of **PPE and 4PP**. Additionally, Figure S5 also indicates that a small peak is present in the Solvo-N_2 sample at the ^{1}t$_R$ and ^{2}t$_R$ of **EV**, indicating the incorporation of the hydrogen donating solvent (ethanol) into the products (**V** in this case) during solvolysis as reported in literature.[33–37] Finally, while Solvo-N_2 and Cata-N_2 display no pronounced selectivity towards a singular peak within the region of low peak density, as expected due to the aforementioned decreased selectivity of solvolysis and catalytic liquid phase reforming,[33–37] Cata-H_2 and Cata-O_2 do display a strong selectivity towards singular peaks within this region (see Figures S2 and S3 in the Supporting Information). More

ChemistryOpen

Full Papers
doi.org/10.1002/open.202100088

Chemistry Europe
European Chemical
Societies Publishing

specifically, Figure S5 in the Supporting Information indicates that **V** is abundantly present in the Solvo-N_2, Cata-N_2 and Cata-O_2 samples, especially within the latter as expected for the mild oxidative depolymerization conditions.[15,22–28] Where the selectivity towards **V** or other important monomers is typically assessed through GC(XGC)-MS/FID, the developed GPC-HPLC-UV/VIS method is also capable of quickly and graphically demonstrating differences in selectivity towards specific interesting products such as **V**.[29] Finally, while Cata-H_2 demonstrates no peaks at the ^1t_R and ^2t_R of **V**, the peak showing the highest intensity in the GPC-HPLC-UV/VIS plot of Cata-H_2 (^{1}D-fraction 4, ^2t_R approx. 5.5 min), is also responsible for the unique peak in the GPC-UV/VIS plot at 21.5 min. This further demonstrates the unique product selectivity within the Cata-H_2 sample.

3. Conclusions

A GPC-HPLC-UV/VIS method has been developed and its feasibility for fast and detailed mapping of lignin depolymerization product pools has been assessed. The technique enables a concise compositional comparison of monomers, dimers and higher molecular weight products, with regards to molecular weight and functionalities, especially OH-groups, which is vital for catalyst development and optimization of reaction conditions. The analysis of a comprehensive standard mixture of lignin-like model compounds revealed distinct selectivity towards the number of OH-groups occurring in both separation dimensions, i.e., a distinct reduction of ^1t_R and ^2t_R. Analysis of real lignin depolymerization samples confirms their inherent complexity in which peak density exponentially increases with hydrodynamic volume, i.e., decreasing ^1t_R, resulting in two distinct zones; one with low peak density and one with high peak density. Differences between samples regarding reaction selectivity are clearly recognized as the occurrence and intensity of peaks in the zone with low peak density, the overall size and position of the zone with high peak density and the nature of the transition between the two zones. Additionally, the GPC-HPLC-UV/VIS method is also capable of quickly assessing differences towards specifically desired products such as vanillin or others. Therefore, the developed technique significantly advances beyond the state-of-the-art and is a valuable tool for catalyst development and optimization of reaction conditions.[46]

Experimental Section

Standard Mixture

To elucidate the effects of molecular structure on both ^1t_R and ^2t_R, a model compound (MC) mixture was prepared and analyzed by means of GPC-HPLC-UV/VIS. The mixture contains 2000 mg/mL of 18 different model components diluted in dimethylsulfoxide (DMSO, Biosolve, 99.9 + %). The molecular structures of all model compounds, categorized into 3 groups, are presented in Figure 1. The first group are phenolics (blue in Figure 1); phenol (Ph, Chem-Lab, 99 + %), resorcinol (R, Chem-Lab, 99 + %), p-cresol (PC, Sigma-

Aldrich, 99 + %), guaiacol (G, Sigma-Aldrich, 99 + %), vanillin (V, Sigma-Aldrich, 99 %) and ethyl vanillin (EV, Sigma-Aldrich, 98.5 %). The second group are eugenolics (green in Figure 1); eugenol (EUG, Sigma-Aldrich, 99 + %), coniferyl alcohol (CA, Alfa Aesar, 98 %), sinapyl alcohol (SA, Sigma-Aldrich, 80 %), trans-ferulic acid (TFA, Sigma-Aldrich, 99 %) and 3-(3-ethoxy-4-methoxyphenyl)-1-propene (EMP, ABCR, 95 %). The third and final group are dimerics (violet in Figure 1); 4-phenoxyphenol (4PP, Sigma-Aldrich, 99 %), benzyl-phenylether (BPE, Alfa Aesar, 97 %), 1-phenyl-2-phenoxyethanol (PPE, AmBeed, 97 + %), guaiacylglycerol-beta-guaiacylether (GG, Sigma-Aldrich, 97 + %), 6,6'-dihydroxy-5,5'-dimethoxybiphenyl-3,3'-dicarbaldehyde (DDC, ABCR, 95 %), 1-(3,4-dimethoxy-phenyl)-2-(2-methoxy-phenoxy)-propane-1,3-diol (DMD, ABCR, 97 %) and combretastatin A4 (COM, Sigma-Aldrich, 98 + %).

Catalyst Preparation

The depolymerization of the Miscanthus lignin is performed in the presence of a, gamma alumina supported, palladium-copper catalyst (PdCu–Al_2O_3). The catalyst is prepared by an incipient wetness impregnation with 0.75 mL of a solution containing 43939 mg Pd^{2+}/L and 26237 mg Cu^{2+}/L per 0.95 g of Al_2O_3. The material is subsequently heated at 2 °C/min to 60 °C, dried at this temperature for 16 h, further heated to 450 °C at 20 °C/min and finally calcined at this temperature for 4 h.

Lignin Stock Solution

The Miscanthus lignin used during the depolymerization experiments was obtained from a pilot scale study published elsewhere.[51] In short, the biomass was fractionated through a mild Soda pulping process after which the lignin was recovered by means of acidification, enzymatic treatment and flocculation. Finally, the obtained lignin was thoroughly characterized via GPC, 2D-HSQC-NMR and 31P-NMR analyses.[51] The stock solution for depolymerization was prepared by dissolving 1.5 g of dried Miscanthus lignin in 10 mL of a 70 vol%/30 vol% ethanol/water mixture, which was stirred at 250 rpm for > 12 h at 25 °C and filtered (grade 1 qualitative Whattman filter).

Reaction Setup and Depolymerization Conditions

The reaction is performed in an Eco-cat 7-25-SS316 reactor supplied by AmAr (Mumbai, India). This setup is comprised of seven individual cylindrical reactor vessels, each with a volume of 25 mL. The reactor vessels can be supplied with pressurized gas independently and can withstand conditions up to 100 bar and 200 °C. Lignin depolymerization is performed by loading 5 mL of a Miscanthus lignin stock solution, 10.5 mL ethanol, 4.5 mL water and 0.1 g PdCu–Al_2O_3 catalyst in a reactor vessel, which is subsequently closed, flushed for 30 seconds with the desired gas, pressurized to 10 bar with that same gas and finally placed within the heating mantle, which is preheated to 200 °C. After 20 h, the catalyst and effluent are separated by filtration (grade 1 qualitative Whattman filter). The mild catalytic depolymerization of the Miscanthus lignin was performed under three different atmospheres, i.e., 10 bar of N_2 (both solvolytic and catalytic, i.e., without and with catalyst), H_2 or O_2. The four resulting product pools are denoted as Solvo-N_2, Cata-N_2, Cata-H_2 and Cata-O_2.

Sample Preparation

To prepare the samples for the 2D-GPC-HPLC analysis, dissolution in the mobile phase of the first dimension, i.e., DMSO + 0.1 vol%

ChemistryOpen

Full Papers
doi.org/10.1002/open.202100088

Chemistry Europe
European Chemical
Societies Publishing

lithium bromide (LiBr, $\geq 99\%$, Sigma-Aldrich) is required. Mixtures of model compounds are directly dissolved within this solvent and, therefore, require no additional sample preparation. The depolymerization effluents are originally dissolved in 70vol%/30vol% ethanol/water, which is removed by evaporation at 80 °C until no liquid is present. Afterwards, the samples are dissolved in a volume of DMSO + 0.1vol% LiBr equal to the original effluent volume that was evaporated.

GPC-HPLC-UV/VIS Analysis

The two-dimensional analyses are performed offline using two Agilent Technology 1260 Infinity II systems. The first system, i.e., ^{1}D, is equipped with an autosampler injecting 80 μL of sample. The stationary phase consists of an Agilent Polargel-L Guard column (50 mm × 7.5 mm ID) and two Agilent Polargel-L columns (300 mm × 7.5 mm ID) in series to increase resolution, all maintained at 65 °C. The mobile phase consists of DMSO with 0.1 vol% of LiBr) and is set at a flow rate of 0.8 mL/min. For the first dimension, a variable wavelength detector (VWD), set to 280 nm at a scan rate of 5 Hz, is used. For the analysis of MCs, eleven fractions of 0.5 min (0.4 mL) are collected from ^{1}D in HPLC vials between a ^{1}t$_R$ of 18 min and 23.5 min. For the analysis of the depolymerization effluents, 19 ^{1}D-fractions of 0.5 min (0.4 mL) are collected between a ^{1}t$_R$ of 14 min and 23.5 min. The fractions are labelled 1 through 11 or 19 in reverse order, i.e., starting with the fraction between 23 min and 23.5 min, as indicated in Figures 3 and 5. The second system, i.e., ^{2}D, is equipped with an autosampler injecting 10 μL of ^{1}D-fraction onto an Agilent Zorbax 300SB-CN column (150 mm × 4.6 mm ID, 3.5 μm particle size) at 45 °C. The mobile phase, set at a flow rate of 1.2 mL/min, consists of water (Chem-Lab, HPLC-grade) with 0.2 vol% acetic acid (Chem-Lab, 99 + %) and acetonitrile (ACN, Chem-Lab, HPLC-grade). The gradient starts at 0 vol% ACN, reaches 2 vol% ACN at 4 min, increases to 30 vol% ACN at 10 min, rises to 70 vol% at 30 min after which it jumps to 100 vol% ACN, which is held for 2 min. Between injections, a post run time of 6 min with 0 vol% ACN is used to re-equilibrate the system. The second dimension also uses a VWD at 280 nm and a scan rate of 5 Hz.

Acknowledgements

Conflict of Interest

The authors declare no conflict of interest.

[1] J. B. Zimmerman, P. T. Anastas, H. C. Erythropel, W. Leitner, *Science* **2020**, *367*, 397–400.

[2] B. A. de Marco, B. S. Rechelo, E. G. Totoli, A. C. Kogawa, H. R. N. Salgado, *Saudi Pharm. J.* **2019**, *27*, 1–8.

[3] H. E. Toraman, R. Vanholme, E. Borén, Y. Vanwonterghem, M. R. Djokic, G. Yildiz, F. Ronsse, W. Prins, W. Boerjan, K. M. Van Geem, G. B. Marin, *Bioresour. Technol.* **2016**, *207*, 229–236.

[4] W. Y. Hernández, J. Lauwaert, P. Van Der Voort, A. Verberckmoes, *Green Chem.* **2017**, *19*, 5269–5302.

[5] L. Dessbesell, M. Paleologou, M. Leitch, R. Pulkki, C. Xu, *Renewable Sustainable Energy Rev.* **2020**, *123*, 109768.

[6] T. De Saegher, J. Lauwaert, J. Hanssen, E. Bruneel, M. Van Zele, K. Van Geem, K. De Buysser, A. Verberckmoes, *Materials* **2020**, *13*, 691.

[7] E. Cooreman, T. Vangeel, K. Van Aelst, J. Van Aelst, J. Lauwaert, J. W. Thybaut, S. Van den Bosch, B. F. Sels, *Ind. Eng. Chem. Res.* **2020**, *59*, 17035–17045.

[8] J. Wildschut, F. H. Mahfud, R. H. Venderbosch, H. J. Heeres, *Ind. Eng. Chem. Res.* **2009**, *48*, 10324–10334.

[9] Z. Sun, B. Fridrich, A. de Santi, S. Elangovan, K. Barta, *Chem. Rev.* **2018**, *118*, 614–678.

[10] A. T. Martínez, F. J. Ruiz-Dueñas, M. J. Martínez, J. C. Del Río, A. Gutiérrez, *Curr. Opin. Biotechnol.* **2009**, *20*, 348–357.

[11] Z. H. Sun, B. Fridrich, A. de Santi, S. Elangovan, K. Barta, *Chem. Rev.* **2018**, *118*, 614–678.

[12] M. S. Ganewatta, H. N. Lokupitiya, C. Tang, *Polymer* **2019**, *11*, 1176.

[13] M. N. Collins, M. Nechifor, F. Tanasa, M. Zanoaga, A. McLoughlin, M. A. Strozyk, M. Culebras, C. A. Teaca, *Int. J. Biol. Macromol.* **2019**, *131*, 828–849.

[14] I. Van Nieuwenhove, T. Renders, J. Lauwaert, T. De Roo, J. De Clercq, A. Verberckmoes, *ACS Sustainable Chem. Eng.* **2020**, *8*, 18789–18809.

[15] W. Schutyser, T. Renders, S. Van den Bosch, S. F. Koelewijn, G. T. Beckham, B. F. Sels, *Chem. Soc. Rev.* **2018**, *47*, 852–908.

[16] H. L. Wang, Y. Q. Pu, A. Ragauskas, B. Yang, *Bioresour. Technol.* **2019**, *271*, 449–461.

[17] L. C. Cao, I. K. M. Yu, Y. Y. Liu, X. X. Ruan, D. C. W. Tsang, A. J. Hunt, Y. S. Ok, H. Song, S. C. Zhang, *Bioresour. Technol.* **2018**, *269*, 465–475.

[18] S. Fadlallah, P. Sinha Roy, G. Garnier, K. Saito, F. Allais, *Green Chem.* **2021**, *23*, 1495–1535.

[19] S. Sarkanen, in *Enzymes in Biomass Conversion, Vol. 460*, American Chemical Society, **1991**, pp. 247–269.

[20] Q. Chen, M. N. Marshall, S. M. Geib, M. Tien, T. L. Richard, *Bioresour. Technol.* **2012**, *117*, 186–192.

[21] L. P. Christopher, B. Yao, Y. Ji, *Front. Energy Res.* **2014**, *2*.

[22] H. H. Luo, L. Y. Wang, G. S. Li, S. S. Shang, Y. Lv, J. Y. Niu, S. Gao, *ACS Sustainable Chem. Eng.* **2018**, *6*, 14188–14196.

[23] V. Tarabanko E, D. Petukhov V, *Chem. Sustainable Dev.* **2003**, 11, 655–667.

[24] P. C. R. Pinto, C. E. Costa, A. E. Rodrigues, *Ind. Eng. Chem. Res.* **2013**, *52*, 4421–4428.

[25] O. Y. Abdelaziz, K. Ravi, F. Mittermeier, S. Meier, A. Riisager, G. Lidén, C. P. Hulteberg, *ACS Sustainable Chem. Eng.* **2019**, *7*, 11640–11652.

[26] S. Kumaravel, P. Thiruvengetam, K. Karthick, S. S. Sankar, A. Karmakar, S. Kundu, *Biotechnol. Prog.* **2021**, *37*, 13.

[27] C. C. Almada, A. Kazachenko, P. Fongarland, D. D. Perez, B. N. Kuznetsov, L. Djakovitch, *Catalysts* **2021**, *11*, 19.

[28] C. Cheng, J. Wang, D. Shen, J. Xue, S. Guan, S. Gu, K. H. Luo, *Polymer* **2017**, *9*, 240.

[29] M. Fache, B. Boutevin, S. Caillol, *ACS Sustainable Chem. Eng.* **2016**, *4*, 35–46.

[30] R. Rinaldi, R. Jastrzebski, M. T. Clough, J. Ralph, M. Kennema, P. C. A. Bruijnincx, B. M. Weckhuysen, *Angew. Chem. Int. Ed.* **2016**, *55*, 8164–8215; *Angew. Chem.* **2016**, *128*, 8296–8354.

[31] C. Xu, R. A. D. Arancon, J. Labidi, R. Luque, *Chem. Soc. Rev.* **2014**, *43*, 7485–7500.

[32] K. M. Torr, D. J. van de Pas, E. Cazeils, I. D. Suckling, *Bioresour. Technol.* **2011**, *102*, 7608–7611.

[33] V. Patil, S. Adhikari, P. Cross, H. Jahromi, *Renewable Sustainable Energy Rev.* **2020**, *133*, 110359.

[34] C. Løhre, H. V. Halleraker, T. Barth, *Int. J. Mol. Sci.* **2017**, *18*, 225.

[35] D. Shen, C. Cheng, N. Liu, R. Xiao, in *Production of Biofuels and Chemicals from Lignin* (Eds.: Z. Fang, J. R. L. Smith), Springer Singapore, **2016**, pp. 289–320.

[36] J. Zakzeski, A. L. Jongerius, P. C. A. Bruijnincx, B. M. Weckhuysen, *ChemSusChem* **2012**, *5*, 1602–1609.

[37] B. Zhang, Z. Qi, X. Li, J. Ji, L. Zhang, H. Wang, X. Liu, C. Li, *Green Chem.* **2019**, *21*, 5556–5564.

[38] A. Lourenço, J. Gominho, H. Pereira, in *Analytical Pyrolysis*, IntechOpen, **2018**, pp. 1–22.

[39] S. Zhan, W. Chenguang, B. Kang, Z. Xinghua, Y. Chiling, R. Dong, M. Longlong, P. Changle, *Int. J. Agric. Biol.* **2017**, *10*, 214–225.

[40] G. H. Wang, X. Q. Liu, J. Y. Zhang, W. J. Sui, J. Jang, C. L. Si, *Ind. Crops Prod.* **2018**, *124*, 216–225.

[41] L. Negahdar, A. Gonzalez-Quiroga, D. Otyuskaya, H. E. Toraman, L. Liu, J. T. B. H. Jastrzebski, K. M. Van Geem, G. B. Marin, J. W. Thybaut, B. M. Weckhuysen, *ACS Sustainable Chem. Eng.* **2016**, *4*, 4974–4985.

[42] T. Sonoda, T. Ona, H. Yokoi, Y. Ishida, H. Ohtani, S. Tsuge, *Anal. Chem.* **2001**, *73*, 5429–5435.

[43] B. C. Owen, L. J. Haupert, T. M. Jarrell, C. L. Marcum, T. H. Parsell, M. M. Abu-Omar, J. J. Bozell, S. K. Black, H. I. Kenttämaa, *Anal. Chem.* **2012**, *84*, 6000–6007.

[44] J. Prothmann, P. Spégel, M. Sandahl, C. Turner, *Anal. Bioanal. Chem.* **2018**, *410*, 7803–7814.

[45] A. S. Ruhl, M. Jekel, *J. Water Supply Res. T* **2012**, *61*, 32–40.

[46] A. Dubuis, A. Le Masle, L. Chahen, E. Destandau, N. Charon, *J. Chromatogr. A* **2020**, *1609*, 460505.

[47] D. R. Stoll, P. W. Carr, *Anal. Chem.* **2017**, *89*, 519–531.

[48] A. Margellou, K. Triantafyllidis, *Catalysts* **2019**, *9*, 43.

[49] J. Zhang, B. Sudduth, J. Sun, Y. Wang, *Catal. Lett.* **2020**, 151, 932–939 .

[50] P. W. Carr, D. R. Stoll, *Two-dimensional liquid chromatography: principles, practical implementation and applications*, Agilent Technologies, Inc., Germany, **2015**.

[51] J. Lauwaert, I. Stals, C. S. Lancefield, W. Deschaumes, D. Depuydt, B. Vanlerberghe, T. Devlamynck, P. C. A. Bruijnincx, A. Verberckmoes, *Sep. Purif. Technol.* **2019**, *221*, 226–235.